

Transport of Water in Small Pores

Shuangyan Xu,^{†,||} Gregory C. Simmons,^{†,⊥} T. S. Mahadevan,[‡] George W. Scherer,^{*,†}
Stephen H. Garofalini,[‡] and Carlos Pacheco[§]

[†]Department of Civil and Environmental Engineering/PRISM, Princeton University, Engineering Quad E-319, Princeton, New Jersey 08544, [‡]Interfacial Molecular Science Laboratory, Department of Materials Science and Engineering, Rutgers University, Piscataway, New Jersey 08855 and [§]Department of Chemistry, Princeton University, Princeton, New Jersey 08544. ^{||} Present address: Applied Materials Xi'an, 28 Xinxu Road, Xi'an Hi-Tech Industrial Development Zone, Xi'an, Shaanxi, P.R. China 710119. [⊥] Present address: 401 E. 34th Street, Apt. S23E, New York, New York 10016-4963.

Received December 10, 2008. Revised Manuscript Received February 11, 2009

Experimental measurements of the thermal expansion coefficient (α), permeability (k), and diffusivity (D) of water and 1 M solutions of NaCl and CaCl₂ are interpreted with the aid of molecular dynamics (MD) simulations of water in a 3 nm gap between glass plates. MD shows that there is a layer ~ 6 Å thick near the glass surface that has $\alpha \sim 2.3$ times higher and D about an order of magnitude lower than bulk water. The measured D is ~ 5 times lower than that for bulk water. However, when the MD results are averaged over the thickness of the 3 nm gap, D is only reduced by $\sim 30\%$ relative to the bulk, so the measured reduction is attributed primarily to tortuosity of the pore space, not to the reduced mobility near the pore wall. The measured α can be quantitatively explained by a volume-weighted average of the properties of the high-expansion layer and the “normal” water in the middle of the pore. The permeability of the porous glass can be quantitatively predicted by the Carman–Kozeny equation, if 6 Å of water near the pore wall is assumed to be immobile, which is consistent with the MD results. The properties and thickness of the surface-affected layer are not affected significantly by the presence of the dissolved salts.

1. Introduction

Transport of aqueous solutions in porous media with nanometric pores is of interest for applications ranging from filtration of water to predicting the durability of concrete. Very good data for the permeability, k , of Vycor glass^{1,2} show that k decreases as the molecular size of the liquid increases; the results could be quantitatively explained by assuming that a monolayer of liquid is immobilized against the pore wall. Recently, molecular dynamics (MD) simulations have been done using a dissociative potential for water that allows reaction with silica to form silanols.^{3,4} When water is introduced into a 3 nm gap between plates of silica glass, the calculated pair distribution functions for oxygen indicate that the structure of water is altered only within about 0.6 nm of the silica surface;⁵ the existence of that layer was shown to account for the anomalously high thermal expansion coefficient of water in porous glasses.^{5,6} If the mobility in that layer is low, then it could also account for the dependence of k on pore size in porous glasses. In the present study, we provide additional data for the mobility of water and aqueous solutions in porous glasses, including measurements of permeability and diffusivity, and interpret the results in light of MD simulations.

2. Experimental Procedure

The porous hosts included rods of Vycor glass (kindly provided by Corning, Inc.) with diameters of ~ 7.2 and 3.4 mm and a silica xerogel with a diameter of ~ 3.4 mm; these materials are identified in ref 6 as “7 nm Vycor”, “5 nm Vycor”, and “Xerogel 3 nm”. (The 5 nm Vycor rods proved to be unsatisfactory for beam bending, because they were geometrically imperfect, but they were used for measurement of diffusivity and thermal expansion.) To remove organic impurities from the pores, the Vycor rods were boiled in a 30% solution of hydrogen peroxide for several hours until the rods turned clear, then rinsed in deionized (DI) water and stored in ethanol. Before measurements, the samples were exchanged into water by submerging them in a volume at least 15 times greater than the volume of rods for at least 12 h. The xerogel rods, which had been prepared from tetramethoxysilane,⁷ were obtained dry and were rehydrated slowly by condensation of water vapor over a period of ~ 4 h (following the method described in ref 8), after which they were stored in DI water. DI water, 1 M NaCl, 1 M CaCl₂, and 1 M MgSO₄ solutions were prepared for both sample types, and a 1 M NaNO₃ solution was prepared exclusively for the Vycor rods. The pH of the MgSO₄ solution was 7, and that of the other solutions was ~ 5.5 ; for some tests, the 1 M CaCl₂ solution was adjusted to pH 2 using hydrochloric acid. That pH was chosen because it is close to the isoelectric point of silica, where the charge on the pore wall is zero; this is expected to reduce the interaction of the wall with dissolved ions.

The three point beam-bending method has been developed to measure the permeability in materials where k is low ($\leq 10^{-18}$ m² ≈ 1 microdarcy).^{2,9,10} The principle of the measurement is that

*Author to whom correspondence should be addressed. E-mail: scherer@princeton.edu.

(1) Debye, P.; Cleland, R. L. *J. Appl. Phys.* **1959**, *30*(6), 843–849.
(2) Vichit-Vadakan, W.; Scherer, G. W. *J. Am. Ceram. Soc.* **2000**, *83*(9), 2240–2245.
(3) Mahadavan, T. S.; Garofalini *J. Phys. Chem. B* **2007**, *111*, 8919–8927.
(4) Mahadavan, T. S.; Garofalini *J. Phys. Chem. C* **2008**, *112*, 1507–1515.
(5) Garofalini, S. H.; Mahadevan, T. S.; Xu, S.; Scherer, G. W. *Chem. Phys. Chem.* **2008**, *9*, 1997–2001.
(6) Xu, S.; Scherer, G. W.; Mahadevan, T. S.; Garofalini, S. H. Thermal Expansion of Confined Water. *Langmuir*, submitted for publication, 2008.

(7) Brinker, C. J.; Scherer, G. W. *Sol-Gel Science*; Academic Press: New York, **1990**.

(8) Scherer, G. W. *J. Non-Cryst. Solids* **1997**, *212*, 268–280.
(9) Scherer, G. W. *J. Non-Cryst. Solids* **1992**, *142*(1–2), 18–35.
(10) Scherer, G. W. *J. Am. Ceram. Soc.* **2000**, *83*(9), 2231–2239; Erratum, *J. Am. Ceram. Soc.* **2004**, *87*(8), 1612–1613.

Table 1. Pore Characterization

| sample ID | surface area ^a (m ² /g) | pore volume ^b (cm ³ /g) | pore diameter ^c (nm) | porosity ^d |
|--------------|---|---|---------------------------------|-----------------------|
| Vycor 5 nm | 179 | 0.204 | 4.55 | 0.305 |
| Vycor 7 nm | 137 | 0.253 | 7.40 | 0.352 |
| Xerogel 3 nm | 628 | 0.370 | 2.85 | 0.425 |

^a Brunauer–Emmett–Teller (BET) surface area. ^b Nitrogen adsorption (cumulative). ^c From nitrogen pore volume, V , and area, A : diameter = $4V/A$. ^d Calculated assuming skeletal density of 2.0 g/cm³ for xerogel and 2.15 g/cm³ for Vycor.

bending a beam of a saturated porous material creates a pressure gradient in the pore liquid, which flows until it equilibrates at atmospheric pressure. The flux of liquid, J , is proportional to the pressure gradient, according to Darcy's law:¹¹

$$J = -\frac{k}{\eta_L} \nabla p \quad (1)$$

where η_L is the viscosity of the pore liquid. The force required to sustain a constant deflection of the beam changes with the pore pressure, and the rate of change of the force can be analyzed to find the permeability. This method was previously used in a study² of a single sample of Vycor with pores 5.4 nm in diameter, with a variety of pore liquids. Details of the theory, experimental setup, test procedure, and data analysis are given in refs 2 and 12. Briefly, a stepper motor (UltraMotion) controls the movement of a load cell that is attached to a pushrod, and a linear variable differential transformer (LVDT, Macro Sensors) with a range of 0–10 mm is mounted around the push rod to detect small displacements. During testing, the sample was seated in a stainless-steel bath and supported by two stainless steel rollers. The sample was completely submerged in the pore liquid throughout the measurement. The position of the LVDT and the applied force were collected by a computer running Workbench PC. The measured load, $W(t)$, is fitted to a theoretical expression,¹⁰ with one of the free parameters being the hydrodynamic relaxation time, τ_R , which is inversely proportional to the permeability.

The self-diffusion coefficient, D , of water in bulk and confined solutions was measured using pulsed field gradient NMR analysis¹³ in a sample of 5 nm Vycor saturated with water or an aqueous solution. One set of samples was prepared by placing the bulk solutions in individual 5 mm NMR test tubes sealed with plastic caps. The other set was formed by taking a 5 nm Vycor sample that had been exchanged in its respective salt solution, wiping excess solution from the surface of the rod and placing the rod in a 5 mm sealed NMR tube. To calibrate the instrument (Varian Inova-500) for diffusion measurements, H₂O with a few drops of D₂O was used ($D = 2.27 \times 10^{-9}$ m²/s at 25 °C was used as diffusivity reference¹⁴). Then the DI water sample and aqueous solutions were placed into the spectrometer to measure the diffusivity for the bulk water molecules. This process was repeated for DI water and aqueous solutions confined in the Vycor.

A gradient magnetic pulse is applied with magnitude G_H and duration δ_H , which imposes a phase on each spin according to the local magnitude of the field. After a time interval Δ , another gradient pulse is applied in the opposite sense, so that it restores stationary spins to their initial condition; however, spins that have diffused from their initial position do not fully reverse their phase at that specific position, along the main axis of the sample, resulting in a magnetic signal decay. The magnitude of the signal is related

to the diffusivity, gradient strength and duration, and the diffusion time by

$$\frac{S(G_H, \Delta, \delta)}{S(0, \Delta, \delta)} = \exp \left[-D(\gamma^2 \delta_H^2 G_H^2) \left(\Delta - \frac{\delta}{3} \right) \right] \quad (2)$$

where S is the signal intensity and γ is the magneto-gyric ratio (42.58 MHz/T). The diffusion time, Δ , was varied to find the asymptotic limit of D for H₂O. (At short times, the molecule moves relatively freely in the liquid in a single pore, but at longer times it begins to meander through the labyrinth of pores. In the limit of long times, it explores a region large enough to contain a representative sample of the whole microstructure.) Measurements were also made on bulk water and aqueous solutions. The diffusivity is found from the slope of a plot of $\ln(S/S_0)$ against $\gamma^2 \delta^2 G_H^2 (\Delta - \delta/3)$. The diffusivity of a fluid confined in a porous network differs from that in the bulk liquid by a factor, τ , called the tortuosity:

$$D_{\text{confined}} = \frac{D_{\text{bulk}}}{\tau} \quad (3)$$

As its name implies, this quantity takes account of the tortuous path that a diffusing molecule must explore as it diffuses; it may also include contributions from time spent adsorbed on the pore walls.¹⁵

The thermal expansion of a series of 1 M salt solutions was measured while the liquids were confined in the pores of the xerogel and Vycor glasses. The method is described in detail in refs 6 and 16. Saturated pieces of the porous glass are placed into a flask with enough extra liquid (identical to the pore solution) to raise the liquid into the neck of the flask. A layer of reflective oil is placed onto the solution to prevent evaporation and to facilitate measurement of the height of the surface by an optical probe. The flask is immersed into a bath whose temperature is adjusted between about 10 and 40 °C, allowing measurement of the thermal expansion coefficient. Since the amount of pore liquid is known (from the weight and porosity of the porous host) and the amount and expansion of the excess (bulk) liquid is also known, it is possible to determine the expansion of the pore liquid.

3. Results

The pore properties found from nitrogen sorption are summarized in Table 1.

Figure 1 shows a series of load relaxation curves from the beam-bending experiments performed on the 7 nm Vycor rods. The load drops rapidly at short times as the pore pressure gradient relaxes; the abrupt bend in the curve occurs

(11) Happel, J.; Brenner, H. *Low Reynolds Number Hydrodynamics*; Martinus Nijhoff: Dordrecht, The Netherlands, 1986.

(12) Vichit-Vadakan, W.; Scherer, G. W. *J. Am. Ceram. Soc.* **2002**, *85*(6), 1537–44; Erratum, *J. Am. Ceram. Soc.* **2004**, *87*(8), 1615.

(13) Zielinski, L. J.; Sen, P. N. *J. Magn. Reson.* **2003**, *165*, 153–161.

(14) Antalek, B. *Concepts in Magn. Reson.* **2002**, *14*, 225–258.

(15) Torquato, S. *Random Heterogeneous Media*; Springer: New York, 2002.

(16) Xu, S.; Simmons, G. C.; Scherer, G. W. Dynamics of Small Confining Systems. In *Materials Research Society Symposium Proceedings*; Fourkas, J. T., Levitz, P., Urbakh, M., Wahl, K. J., Eds.; Materials Research Society: Warrendale, PA, **2004**; Vol. 790, P.6.8.1–7, pp 85–91.

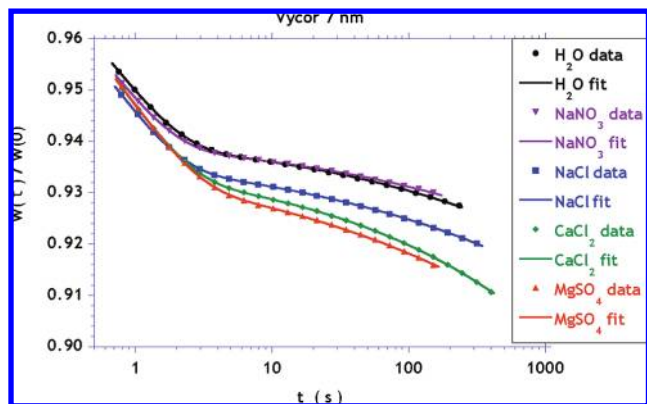


Figure 1. Relaxation of load, $W(t)$, measured on 7 nm Vycor rods containing pure water or 1 M solutions of various salts.

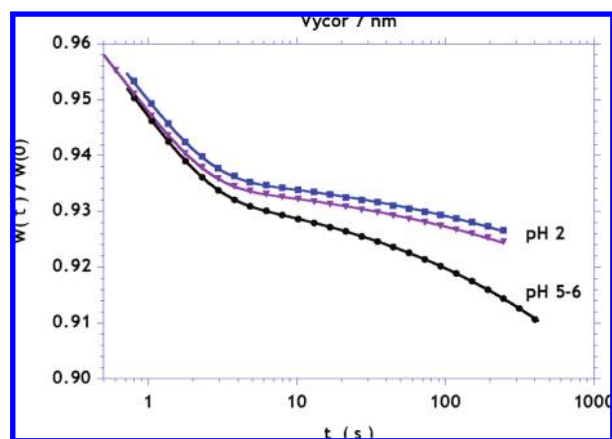


Figure 2. Relaxation of load, $W(t)$, measured on 7 nm Vycor rods containing 1 M solutions of CaCl_2 with the pH adjusted to 2 (upper two curves) or not.

near $t/\tau_R \approx 0.2$ (where $\tau_R \approx 12\text{--}15$ s in these samples), and indicates that the pore liquid has reached atmospheric pressure. The subsequent relaxation results from the viscoelasticity of the solid phase of the porous glass, as has been discussed elsewhere.^{2,17} As shown in Figure 2, the viscoelastic relaxation is slower at pH 2, where the rate of hydrolysis of siloxane bonds is minimal; however, the hydrodynamic relaxation time is not significantly affected. A similar effect has been seen in silica gels subjected to bending in solutions with a range of pH.¹⁷ The amount of relaxation that has occurred at the point where the bend in the curve appears is related to the compressibility of the pore liquid: the more the liquid resists the imposed strain, the greater the pressure that develops in the liquid, and the greater the relaxation as the pore pressure equilibrates. The results of the beam-bending measurements are summarized for the 7 nm Vycor and 3 nm Xerogel samples, in Tables 2 and 3, respectively.

Results of the NMR measurements are presented in Table 4. The self-diffusion coefficient of water in the pores of the 5 nm Vycor is slower than in bulk liquid by about a factor of 5, and is only slightly affected by the presence of 1 M NaCl, but the effect is somewhat greater in 1 M CaCl_2 . This value for the

tortuosity is consistent with previously published values for pure water in porous glass.^{18–20}

The effect of confinement on the volumetric thermal expansion coefficient, α , is illustrated in Figure 3. The dashed curve shows that α for water confined in 7 nm Vycor is about 25% higher than for bulk water. The enhancement in α increases as the temperature decreases, because α drops to zero in pure water at 4 °C, while α for confined water remains finite (so the ratio would diverge at 4 °C). At 20 °C, α is about 1.5 times as large for a bulk solution of 1 M NaCl as for pure water; the same ratio applies for the ratio of those liquids confined in the pores of 7 nm Vycor. Therefore, the effect of confinement on α is not significantly influenced by the presence of NaCl. The effect of 1 M CaCl_2 is slightly greater, but still is only on the order of 10%. In both cases, the ratio α (solution)/ α (water) rises less rapidly at low temperatures for the confined liquids, because α for confined water drops to zero at a temperature well below 4 °C.⁶

4. Molecular Dynamics

The MD computer simulations employed a recently developed dissociative water potential³ in conjunction with a silica version of the same form that has previously been used to simulate the interactions between silica and water vapor⁴ and the thermal expansion of nanoconfined water.⁵ The system used in the current simulations of diffusion of nanoconfined water is similar to that used previously.⁵ Briefly, 11664 atoms of Si and O were used to create the silica glass in a box ~ 6.4 nm \times 6.4 nm \times 4.3 nm with periodic boundaries using a melt-quench procedure starting at 6000 K and cooling to 4000, 3000, 2000, 1000, and 298 K under NVE (constant number, volume, energy) conditions for a total of 430 000 steps, with a time step of 1 fs. In these NVE runs, the volume was changed as a function of temperature, based on the thermal expansion coefficient of silica, so that the final glass had a density of 2.2 g/cm³. This glass was then equilibrated at 298 K in a 40 ps NPT (constant number, pressure, temperature) run with a hydrostatic pressure of 1 atm. A slab of water ~ 3 nm thick, containing 4851 water molecules, was placed in contact with the silica, with periodic boundaries, causing the water to be confined between silica surfaces. The total system was run under modified NPT simulations, in which the x and y dimensions were kept constant and a 1 atm pressure was applied in the z dimension. The system was run for 2 000 000 moves at 298 K using a time step of 0.1 fs.

The density profile of ions in the system was made from the final 600 000 moves in order to distinguish water at the interface from water in the interior of the film for subsequent diffusion analysis. The density profile is shown in Figure 6.

The data for the diffusion coefficients were taken from the mean square displacement (MSD) of the O ions in the water molecules during the last 1.0×10^6 moves of the 2.0×10^6 move run. These O ions exclude those O from water that chemisorbed onto the silica surface during the formation of silanols (SiOH). MSDs are taken over all remaining water (labeled “All”), over all water in the interior of the film (~ 9 Å from either interface and labeled “interior”), and in 6 Å thick “layers” parallel to the interface as a function of distance (Z) from the lower interface. The MSDs in the “layers” are taken in two and three dimensions, which are in XY and XYZ , respectively.

(17) Scherer, G. W. *Faraday Disc.* **1995**, *101*, 225–234.

(18) Lin, M. Y.; Abeles, B.; Huang, J. S.; Stasiewski, H. E.; Zhang, Q. *Phys. Rev. B* **1992**, *46*(1), 10701–10705.

(19) Levitz, P. In *Handbook of Porous Media*; Sing, K., Ed.; Wiley-VCH: Weinheim, Germany, **2002**; Vol. 1, pp 37–80.

(20) Scherer, G. W.; Valenza II, J. J.; Simmons, G. *Cem. Concr. Res.* **2007**, *37*, 386–397.

Table 2. Parameters from Beam-Bending Measurements on 7 nm Vycor

| | 7 nm Vycor | | | | | |
|---------------------------------------|-----------------|-------------------|-------------|-------------------|------------------------|-------------------|
| | water | NaNO ₃ | NaCl | CaCl ₂ | CaCl ₂ pH 2 | MgSO ₄ |
| # of runs | 3 | 2 | 2 | 4 | 3 | 3 |
| η_L (mPa·s) | 1.002 | 1.059 | 1.097 | 1.331 | 1.331 | 1.946 |
| K_L (GPa) | 2.18 | 2.48 | 2.53 | 2.71 | 2.71 | 2.90 |
| K/η_L (nm ² /Pa·s) | 211 ± 1.5 | 198 ± 12 | 188 ± 4.9 | 154 ± 16 | 148 ± 2.9 | 116 ± 6.2 |
| E_p (GPa) | 13.7 ± 0.04 | 14.2 ± 0.06 | 13.7 ± 0.1 | 14.0 ± 0.2 | 13.5 ± 0.3 | 12.9 |
| A | 0.0572 ± 0.0006 | 0.0513 ± 0.0097 | 0.0601 ± 0 | 0.0545 ± 0.0077 | 0.0576 ± 0.0063 | 0.0573 ± 0.0020 |
| τ_R (s) | 13.6 ± 0.1 | 12.4 ± 0.03 | 13.5 ± 0.4 | 15.1 ± 1.2 | 15.5 ± 0.5 | 18.9 ± 0.7 |
| η_{soln}/η_{water} (bulk) | 1.00 | 1.06 | 1.09 | 1.33 | 1.33 | 1.94 |
| η_{soln}/η_{water} (confined) | 1.00 | 1.07 | 1.12 ± 0.31 | 1.38 ± 0.095 | 1.42 | 1.81 |

Table 3. Parameters from Beam-Bending Measurements on Xerogel

| | 3 nm Xerogel | | | | |
|---------------------------------------|-----------------|-----------------|-------------------|------------------------|-------------------|
| | water | NaCl | CaCl ₂ | CaCl ₂ pH 2 | MgSO ₄ |
| # of runs | 4 | 4 | 4 | 3 | 4 |
| η_L (mPa·s) | 1.002 | 1.097 | 1.331 | 1.331 | 1.946 |
| K_L (GPa) | 2.18 | 2.53 | 2.71 | 2.71 | 2.90 |
| k/η_L (nm ² /Pa·s) | 22.2 ± 0.1 | 19.6 ± 0.4 | 15.4 ± 0.6 | 21.1 ± 0.4 | 13.1 ± 0.4 |
| E_p (GPa) | 4.06 ± 0.07 | 4.17 ± 0.02 | 4.68 ± 0.08 | 4.61 ± 0.06 | 4.57 ± 0.06 |
| A | 0.0953 ± 0.0014 | 0.0957 ± 0.0011 | 0.0910 ± 0.0018 | 0.0903 ± 0.0009 | 0.0857 ± 0.0009 |
| τ_R (s) | 45.4 ± 0.7 | 44.2 ± 0.8 | 50.0 ± 1.7 | 36.0 ± 0.3 | 49.9 ± 1.2 |
| η_{soln}/η_{water} (bulk) | 1.00 | 1.09 | 1.33 | 1.33 | 1.94 |
| η_{soln}/η_{water} (confined) | 1.00 | 1.13 | 1.44 | 1.05 | 1.70 |

Table 4. Self-Diffusion Coefficient of Water (m²/s) Found by NMR

| | water | 1 M NaCl | 1 M CaCl ₂ |
|---|-------|----------|-----------------------|
| D (bulk) (10 ⁻⁹ m ² /s) | 2.27 | 2.08 | 1.99 |
| D (confined) (10 ⁻⁹ m ² /s) | 0.464 | 0.425 | 0.339 |
| D^{water}/D^{soln} (bulk) | | 1.09 | 1.14 |
| D^{water}/D^{soln} (confined) | | 1.09 | 1.37 |
| D (bulk)/ D (confined) | 4.89 | 4.89 | 5.87 |

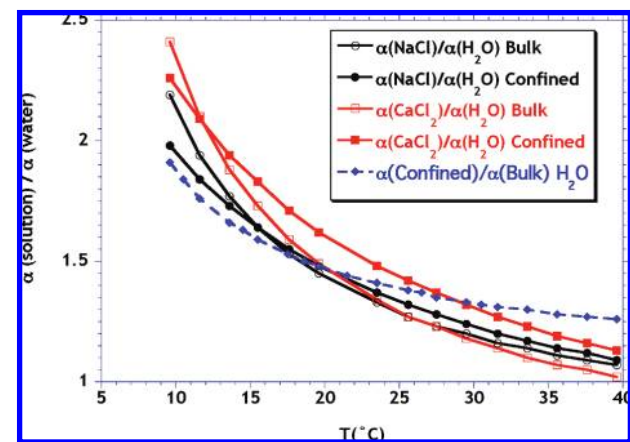


Figure 3. Solid curves show ratio of volumetric thermal expansion coefficient, α , of 1 M solution to that of pure water for bulk solutions (Bulk) and for solutions confined in the pores of 7 nm Vycor (Confined). Dashed curve shows ratio of α for pure water confined in 7 nm Vycor to that for bulk water.

The MSD data were collected over the final 90 ps of the run. The MSD, $\overline{r_t^2} = \langle (r(t) - r(t_0))^2 \rangle$ was averaged over 50 initial configurations, t_0 , each separated by 1.0 ps, and $\tau = t_0 + t$. Time t was taken for all subsequent configurations up to a total of 40 ps from each t_0 . MSD data were collected in these “layers” for O only, while the O was within the selected Z

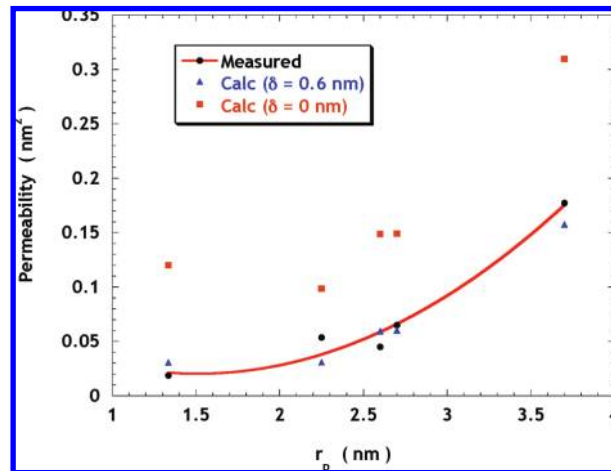


Figure 4. Permeability measured in porous glasses with various pore radii, r_p . Circles are measured values, and triangles are calculated from the Carman–Kozeny equation assuming that the thickness of the immobile layer is $\delta = 0$ (Δ) or 0.6 (\blacktriangle) nm.

dimension. If it moved out of the dimensional limits, it was no longer included. However, if it came back in, the re-entry initiated a new t_0 start for subsequent behavior in the “layer”. The diffusion coefficient, D , was then calculated from the slope of $\overline{r_t^2}$ as a function of elapsed time using

$$D = \frac{1}{2\beta} \left(\frac{d\overline{r_t^2}}{dt} \right) \quad (4)$$

where β represents the dimensionality of the diffusion.

The MSD data are given in Figures 7–9. Figure 7 shows the three-dimensional MSD for all O in water that has not chemisorbed (labeled “All”) and water between 29 and 45 Å in the interior of the film. All MSD data of water excludes

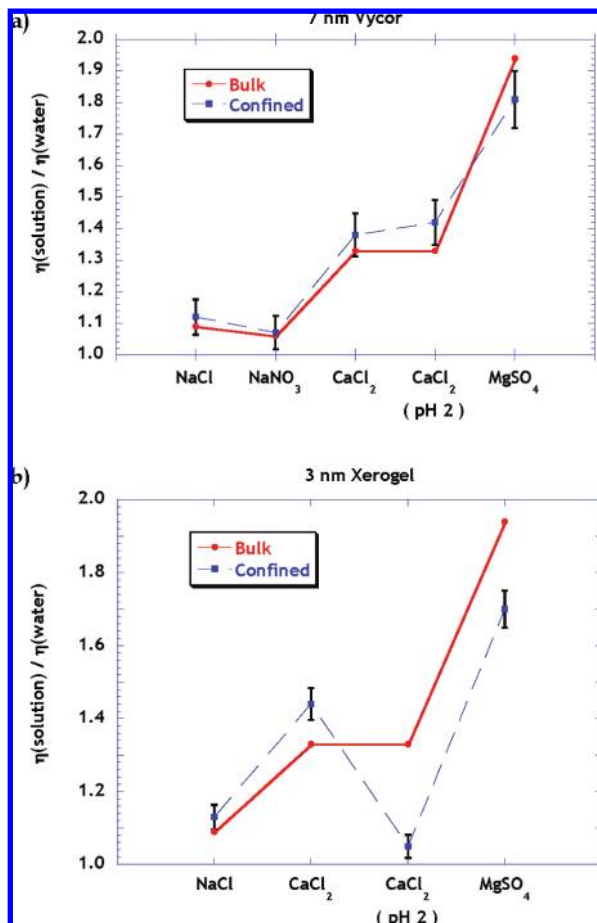


Figure 5. Ratio of viscosity of 1 M solutions to that of water for bulk solutions and for liquids confined in (a) 7 nm Vycor or (b) 3 nm Xerogel. Error bars are standard deviations based on a range of measured values.

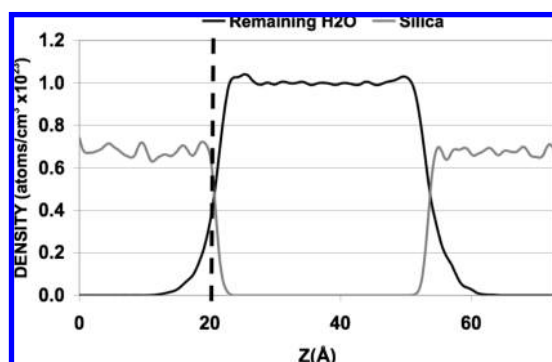


Figure 6. Density profile of silica and “remaining water”, which is the nonchemisorbed water.

chemisorbed oxygen. From the slopes of these lines, diffusion in the interior of the film ($2.1 \times 10^{-5} \text{ cm}^2/\text{s}$) is only slightly lower than that of normal bulk water ($D_B = 2.3 \times 10^{-5} \text{ cm}^2/\text{s}$)²¹ and our previous MD simulations of diffusion in bulk water ($2.4 \times 10^{-5} \text{ cm}^2/\text{s}$).³ The value of D for “All” is $1.6 \times 10^{-5} \text{ cm}^2/\text{s}$, a decrease of $\sim 30\%$ from bulk water. The decrease in the MSD for “All” in Figure 7 can be attributed mostly to the water near the interface for O with $Z > 20 \text{ \AA}$;

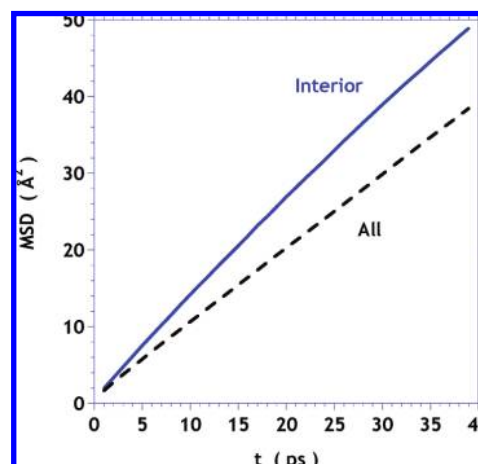


Figure 7. Three-dimensional MSD versus time in picoseconds for all remaining oxygen in water (All) and water between 29 and 45 Å (Interior).

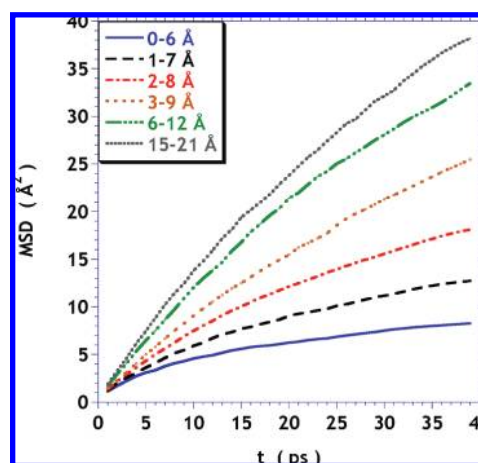


Figure 8. Three-dimensional MSD versus time in picoseconds for water in slices 6 Å thick, taken parallel to the glass surface over the indicated distances. In this plot, 0 Å corresponds to the dashed line in Figure 6, so 15–21 Å is near the middle of the gap between the glass plates.

the few water molecules below the interface make a small contribution to the decrease. Figure 8 shows the significantly lower displacement of O at the interface (0–6 Å from the interface, where the interface is indicated by the vertical dashed line at 20 Å in Figure 6). The curvature of the lines is caused by the inclusion of the Z dimension in the data (diffusion in X , Y , and Z). When the MSD is calculated in two dimensions by taking account only of displacements parallel to the interface (X and Y), the MSD–time plots are nearly linear, as shown in Figure 9. Using the slope of a linear fit to the data in Figure 9 for the slice lying 15–21 Å from the surface, with $\beta = 2$ in eq 4, gives $D = 2.3 \times 10^{-5} \text{ cm}^2/\text{s}$, in agreement with the bulk diffusivity, D_B . A similar fit to the slice at 0–6 Å over the last 20 ps indicates a diffusivity of $\sim D_B/8$. A volume-weighted average in which 6 Å slices at the glass surface have diffusivity $D_B/8$ and the rest of the film has diffusivity D_B yields an average of $1.5 \times 10^{-5} \text{ cm}^2/\text{s}$, which agrees well with D for “All”.

A preliminary simulation was performed to find the diffusivity of water in a cylindrical pore in amorphous silica with a diameter of 3 nm and a length of 3.5 nm. The average diffusion coefficient for all the water molecules was equal to 1.1×10^{-5}

(21) Eisenberg, D.; Kauzmann, W. *The Structure and Properties of Water*; Oxford University Press: London, 1969.

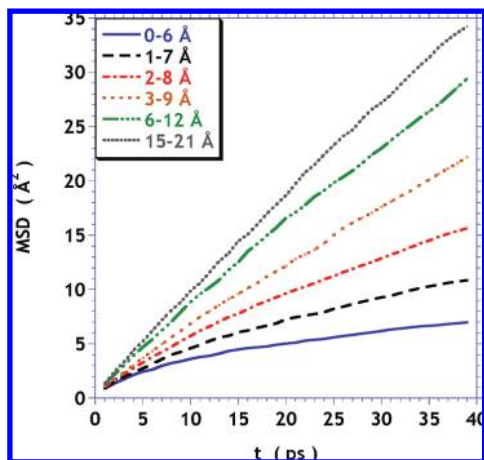


Figure 9. Two-dimensional MSD versus time in picoseconds for water in slices 6 Å thick, taken parallel to the glass surface over the indicated distances. In this plot, 0 Å corresponds to the dashed line in Figure 6, so 15–21 Å is near the middle of the gap between the glass plates. This plot differs from that in Figure 8 in that it only includes displacement parallel to the glass plate.

cm^2/s .²² This is very close to the result (viz., $1.0 \times 10^{-5} \text{ cm}^2/\text{s}$) of a volume-weighted average in which the outer 6 Å of the cylinder has diffusivity $D_B/8$ and the remaining liquid has D_B . The same calculation for a cylinder 5 nm in diameter yields $D = 1.5 \times 10^{-5} \text{ cm}^2/\text{s}$, which is about the same as in a 3 nm film.

5. Discussion

Debye and Cleland¹ found, using conventional flow-rate measurements, that the permeability decreased systematically as the size of the molecule of the pore liquid increased; they attributed the effect to a monolayer of immobile liquid on the pore wall that reduced the effective pore size. In agreement with that idea, Vichit-Vadakan and Scherer² found that they could account for the observed permeability of Vycor (with 5.4 nm pore diameter) by using the Carmen–Kozeny equation:¹¹

$$k = \frac{\phi r^2}{4\kappa} \quad (5)$$

where ϕ = porosity, r = pore radius, and κ = Kozeny “constant” which is slightly dependent on density.²³ To explain the variation in k with molecular size, they assumed that the mean pore size and pore volume measured by nitrogen desorption were reduced by the thickness of a single monolayer of liquid.² Apart from the immobile layer, the pore liquid was assumed to have its normal viscosity. The liquid that gave the poorest agreement in that calculation was water. Since our recent MD simulations^{5,6} indicate that the structure of water is strongly affected over a distance about 0.6 nm (or, about two molecular diameters) from the silica surface, we have repeated the calculation of permeability assuming that the immobile layer is 0.6 nm thick. Figure 4 shows results for a series of porous glasses (including the xerogel and Vycor samples from the present study and the Vycor used in ref 2) containing water. The calculated and measured permeabilities are in reasonable agreement, if we assume that the thickness of the immobile layer, δ , is ~ 2 monolayers ($\delta = 0.6 \text{ nm}$), but not if that layer is neglected ($\delta = 0$).

The beam-bending measurement yields the quantity k/η_L . If we perform beam-bending on a porous glass containing pure water, then exchange the liquid for a salt solution, the pore structure does not change. Assuming that δ is not significantly changed by the presence of salt, then k is the same for both samples, and we can find the enhancement of η_L caused by confinement from the ratio of the measured quantities:

$$\frac{(k/\eta_L)_{\text{water}}}{(k/\eta_L)_{\text{solution}}} = \left(\frac{\eta_L^{\text{solution}}}{\eta_L^{\text{water}}} \right)^{\text{confined}} \quad (6)$$

If this value is different from the viscosity ratio for the bulk liquids, then confinement affects the solution differently from pure water. The results presented in Figure 5 show that the effect of confinement is the same, within experimental uncertainty, for the solutions and for pure water. This implies that the thickness of the layers immobilized on the wall is not significantly affected by the presence of the salts at neutral pH. The only solution that does behave differently is the 1 M CaCl_2 with a pH of 2 confined in the 3 nm Xerogel. This may indicate that the surface-affected layer is more mobile or less thick when the surface charge on the wall is eliminated; however, the change must be modest, because Figure 4 shows that elimination of the immobile layer would raise the permeability by about a factor of 5, whereas the reduction indicated in Figure 5b is less than a factor of 2.

The self-diffusion coefficient measured in bulk water by NMR agrees well with the handbook value.^{21,24} The results presented in Table 4 show that the ratio of D in pure water to that in a solution is about the same in the small pores as in bulk liquid, so ion size does not seem to have much effect on mobility in pores of this size. Comparing D for a given liquid in bulk and confinement indicates a 5-fold decrease, which results from the tortuosity of the pore network, as well as any changes in mobility. The MD simulations show that the diffusion coefficient is about an order of magnitude lower within 6 Å of the glass surface, but the average diffusivity in the pore (given by the curve labeled “All” in Figure 7), differs by $\sim 30\%$ from the bulk diffusivity. Simulations of water confined to a 3 nm cylindrical pore in silica resulted in a similar change in D when the average for all water is considered. Therefore, the low value of D obtained from NMR results primarily from the tortuosity of the pore network, not from reduced mobility of the molecules near the wall.

Our results for viscosity, diffusivity, and permeability are consistent with the widely accepted view that the structure of pore liquid is strongly modified only in the immediate vicinity of the pore wall. That is, the mobility is very low for one or two monolayers, and the rest of the liquid has properties similar to bulk. However, the change in thermal expansion coefficient of the confined liquid is surprisingly large.^{6,16,25} MD simulations reported previously⁵ show that there is a layer within 6 Å of the glass surface where the volumetric thermal expansion is $\sim 5.9 \times 10^{-4} \text{ }^\circ\text{C}^{-1}$, which is ~ 2.3 times that of bulk water. Taking account of the properties of that layer, and assuming that the remainder of the pore liquid is bulk water, the observed thermal expansion of confined water can be semi-quantitatively predicted.⁶ As discussed previously,^{5,6} the interfacial water has a higher density structure that is consistent

(24) Weast, R. C.; Astle, M. J. *CRC Handbook of Chemistry and Physics*, 62nd ed.; CRC Press: Boca Raton, FL, 1981.

(25) Derjaguin, B. V.; Karasev, V. V.; Khromova, E. N. *J. Colloid Interface Sci.* **1986**, *109*(2), 586–587.

(22) Lockwood, G.; Garofalini, S. H.; Scherer, G. W., in preparation.

(23) Scherer, G. W. *J. Sol-Gel Sci. Technol.* **1994**, *1*, 285–291.

with water at a higher pressure. The thermal expansion coefficient of water at elevated pressure is higher than that of water at 1 atm pressure,²⁶ providing the contribution to the confined water's higher expansion. Comparing the curves for confined and bulk solutions in Figure 3, it is apparent that the presence of the salt does not have a large effect on the enhancement of the thermal expansion. According to the MD study conducted by Kohlmeyer, et al.,²⁷ strong attractions between hydrated ions and the solid surfaces can enhance the orientational order of water near the solid surface. Therefore, the divalent ion Ca^{2+} would be expected to be a stronger structure modifier for confined water near the pore wall than the monovalent Na^+ . Although the diffusivity is more strongly influenced by Ca^{2+} than Na^+ , the effect is modest for all the properties examined in this study.

Conclusions

We have measured the permeability, diffusivity, and thermal expansion coefficient of water and aqueous solutions (1 M NaCl and CaCl_2) in porous glasses with pore diameters ranging from 2.85 to 7.4 nm. To help in the interpretation of the results, we have used MD simulations to investigate the thermal expansion and diffusivity of water in a 3 nm gap between glass plates. The measured diffusivity of the liquid confined in 5 nm pores is reduced by about a factor of

5 compared to bulk liquid. MD simulations show that the mobility is reduced by about an order of magnitude within 6 Å of the surface, but when averaged over the 3 nm gap, the diffusivity is only about 30% lower than the bulk value; a similar value is expected in a 5 nm cylinder. This shows that the reduction in measured diffusivity is not simply a consequence of the low mobility near the pore wall, but results primarily from the tortuosity of the pores. MD simulations also show that the layer of water within 6 Å of the pore wall has a high thermal expansion coefficient. Using a simple volume average to take account of the influence of that layer, we can semiquantitatively account for the high values of thermal expansion observed in confined water and solutions. The permeability of porous glass has been reported to depend on the molecular size of the pore liquid, and this effect has been attributed to a relatively immobile layer of molecules on the pore wall. Our experimental results are consistent with the existence of a highly viscous layer ~ 6 Å thick on the pore wall, and the existence of such a layer is quantitatively supported by the MD simulations. The presence of 1 M NaCl has no significant effect on these results, and 1 M CaCl_2 has a very small effect, so the thickness of the surface-affected layer is not strongly affected by the presence of the hydrated ions.

Acknowledgment. The authors are indebted to Dr. Paul Danielson (Corning, Inc.) for providing the porous Vycor glass used in this study. This work was supported by DOE contract DEFG 02-97ER45642.

(26) Minassian, L. T.; Pruzan, P.; Soulard, A. *J. Chem. Phys.* **1981**, *75*, 3064–3072.

(27) Kohlmeyer, A.; Hartnig, C.; Spohr, E. *J. Mol. Liq.* **1998**, *78*, 233–253.